Bandstructure analysis of Sub-Wavelength Grating Waveguide

A Project Report

submitted by

B MEENA

in partial fulfillment of the requirements

for the award of the degree of

MASTER OF TECHNOLOGY

DEPARTMENT OF ELECTRICAL ENGINEERING

INDIAN INSTITUTE OF TECHNOLOGY MADRAS.

May 2018

THESIS CERTIFICATE

This is to certify that the thesis titled **Band Structure analysis of Sub-Wavelength Grating waveguide** , submitted by **B MEENA** bearing Roll number **EE17M067**, to the Indian Institute of Technology, Madras, for the award of the degree of **Master of Technology**, is a bona fide record of the research work done by him under our supervision. The contents of this thesis, in full or in parts, have not been submitted to any other Institute or University for the award of any degree or diploma.

Dr. Bijoy Krishna Das
Project Guide
Professor
Dept. of Electrical Engineering
IIT-Madras, 600 036

Place: Chennai, India

Date: Thu 10th May, 2018

Dedicated to my Parents and Friends...

ACKNOWLEDGEMENTS

First of all, I would like to sincerely thank my guide Dr. Bijoy krishna Das for his valuable technical guidance as well as for the much needed encouragement and support. It has been a great opportunity working under him and this work would not have been possible if not for his vast expertise in the area of Opto-electronics.

I am very thankful to each and every member of the Integrated Optoelectronics group for their valuable support during the course of my work. Their support and immense knowledge in Silicon Photonics helped me for the successful completion of the thesis. I would like to thank all the members of the MEMS lab where i have done my fabrication for their help and support during the project.

Special thanks to Sumi R, Riddhi Nandi and for rendering their help and support. I am very grateful to them for teaching and training me the simulation. I express my sincere gratitude to Arnab, Sreevatsa Kurudi, Parimal Sah who are the members of Integrated Optoelectronics team for giving good motivation and suggestions in the group discussions and also helping me in various stages of my project work.

I would like to thank the Department of Electrical Engineering, IIT Madras for offering the most comprehensive curriculum, and for encouraging the students to work in an area of their interest. I would like to thank the Head of the Department [write your hod name here] and all the faculty members of the department. Last but not the least, I would also like to thank my friends and family members for their continued support during the course of this work.

ABSTRACT

Light propagation in SWG devices is studied and realized with no cladding on top of the waveguide and design of silicon on insulator (SOI) sub-wavelength grating (SWG) for broadband spectrum is been achieved. In particular, we focus on SWG taper with change in parameters like period (Λ), duty cycle (δ), and taper length. The change in period with existing SWG waveguide device results Fabry-Perot resonance due to taper response and further the results are compared with the simulation results of structure where no taper is present (called abrupt transition structure) which conclude that the SWG taper act as reflector.

The proposed structure works on neglecting as well as maximizing the resonance response by changing parameter of SWG. The shorter taper length with higher duty cycle of SWG give high quality factor (Q) and longer taper length with higher duty cycle give sharp left edge pass band which can be used for filter application. Therefore variation of duty cycle of grating have higher impact in taper reflection and transmission region. Bandstructure plot for variation of duty cycle to lead to deeper understanding of photonic band region and transmission region

TABLE OF CONTENTS

LIST OF FIGURES

ABBREVIATIONS

Acronyms

CMOS	Complementry Metal Oxide Semiconductor
SWG	Sub-wavelength grating
Q	Quality factor
F-P	Fabry-Perot
SOI	Silicon-On-Insulator
TE	Transverse Electric (polarization)
TM	Transverse Magnetic (polarization)

Units

dB	decibel
dBm	decibel milli-watt
mW	milli watt
μ**m**	micro meter

NOTATIONS

$\mathbf{n}$	Refractive index
$\mathbf{n}_{eff}$	Effective refractive index
$\boldsymbol{\epsilon}$	Permitivity
$\boldsymbol{\lambda}$	Wavelength
$\boldsymbol{\beta}$	Propagation constant
$\boldsymbol{\phi}$	Phase of the EM wave
$\mathbf{L}$	Length (refers to device length, component length)
$\boldsymbol{\Gamma}$	Overlap integral coefficient
$\boldsymbol{\alpha}$	Loss per unit length

CHAPTER 1

Introduction

1.1 Background

Electronics plays a major role in our day to day life and different areas of science and technologies like Telecommunications, High speed computing, Instrumentation, Biomedical and Sensing. Invention of integrated chips(IC) marked the evolution of electronics. The development of compact and high speed devices could be attributed to the invention of ICs. The development of CMOS fabrication technology lead to the phenomenal development in electronics industry. The need for high speed and compact devices increased gradually and the density of transistors also increased exponentially. As the transistor size is scaling down, its speed and integration density is following Moore's law [1]. But, the interconnect delay is significantly higher when the metal interconnects from device to device or chip to chip are scaled down to submicron regime. At higher operating frequencies, the down scaled metal lines exhibit higher resistance and capacitance which in turn increases the RC time delay; resulting into an over-all limitation in microprocessor speed and the bandwidth. And the power dissipation is also exponentially increased.

It is identified that the interconnect delay can be reduced by replacing electronic interconnects by optical interconnects. Optical interconnects can increase the speed as well as the bandwidth of the devices. Compatibility with existing CMOS fabrication technology, energy efficiency, high speed optoelectronics conversion and higher integration density are the basic requirements for an optical interconnect. These demands push towards to a default solution to use Silicon for photonics circuits too. Since the bandgap of Silicon is $1.12eV$, it is transparent to the IR and MIR wavelengths which are used for optical communication. Another advantage of silicon (with air or SiO_2 as cladding) is its high refractive index contrast which will help us to integrate compact

photonics circuits within a chip. It can be integrated with electronics in the same device layer using the same process flow as for CMOS electronics.

1.2 Sub-wavelength grating waveguide

In integrated photonic circuits, the refractive index contrast is usually set by the choice of the material platform. For example, for silicon photonic circuits the waveguide core and the cladding indices are given by the material constants of silicon (nSi = 3.47) and silicon dioxide (nSiO2 = 1.44) and waveguide devices must be designed within the constraint of these fixed values . By having periodic dielectric structures with a periodicity smaller than one half of the wavelength do not diffract any light. These are called subwavelength gratings (SWGs) and act as homogeneous effective media with spatially averaged refractive index.

1.3 Application of SWG regime

One of the fundamental building blocks, using sub-wavelength structures, is the sub-wavelength grating (SWG) waveguide. Scanning electron microscope (SEM) images of an SWG waveguide and an SWG waveguide taper . A theoretical study has confirmed that the SWG waveguide is lossless in the absence of fabrication imperfections [69]. As compared to the conventional silicon wire waveguides, SWG waveguides provide some features that are beneficial in specific applications. Due to the fact that SWG waveguides consist of rectangles with alternating indices, SU- 8 polymer has been used as the cladding material to make athermal SWG waveguides []. Due to the fact that SU-8 has a negative thermo-optic coefficient while silicon has a positive thermo-optic coefficient, a athermal SWG waveguide can be created by interleaving specific amounts of these two materials. Silicon oxide is normally used as the cladding material for SOI devices, and the material dispersion of silicon oxide is 6X lower than in silicon. Therefore, SWG waveguides are less wavelength dependent than silicon waveguides. Experimental demonstration of SWG waveguide, which has propagation loss as low as 2:1 dB=cm with negligible polarization and wavelength dependent loss has been

demonstrated in []. In addition, SWG waveguides also have a much smaller effective indices as compared to the conventional silicon wire waveguide. The reduced effective indices leads to loosely conned optical modes in the waveguides, which are ideal for applications such as bio-sensing []. Sub-wavelength structures have also been used to optimize grating couplers. When combining fundamental building blocks that can be fabricated in a single, fully-etched step, having fully-etched sub-wavelength grating couplers (SWGCs) provides an efficient and economical solution for rapid prototyping.

1.4 Research Objective

The key objective of my work is to understand the bandstructure of SWG waveguide and taper design, Change in SWG parameter affects the transmission spectra through taper reflection which is observed in existing SWG waveguide design. Hence my work will focus on design and simulate a SWG structure to over come the loss from taper due to change in parameter SWG

1.5 Thesis Organization

The thesis is organized in four chapters. First chapter gives an introduction to Silicon Photonics and SWG waveguide. It also discusses various ongoing research works in this field and motivation that lead to do this research. The second chapter discusses the theoretical background period dielectric structure which leads to understand the light guidance in Sub-wavelength grating structure. The simulation results on proposed structure with varying parameter are discussed in the third chapter. In the final chapter, the summary of the project and outlook has been discussed in brief.

CHAPTER 2

Background Theory

2.1 Fundamentals of 1D periodic medium

Light propagation in periodic arrangements of high and low refractive index material can be understood from 1D dispersion curve as shown in figure 2.1, generally operates in the following three regimes, depending on the ratio between structures period Λ and the operating wavelength λ:

(i) Diffraction regime. The incoming beam is scattered in different orders

(ii) Bragg reflection regime. The incoming beam is reflected backward

(iii) Sub-wavelength regime. The diffraction and reflection effects due to periodicity of the structure are suppressed.

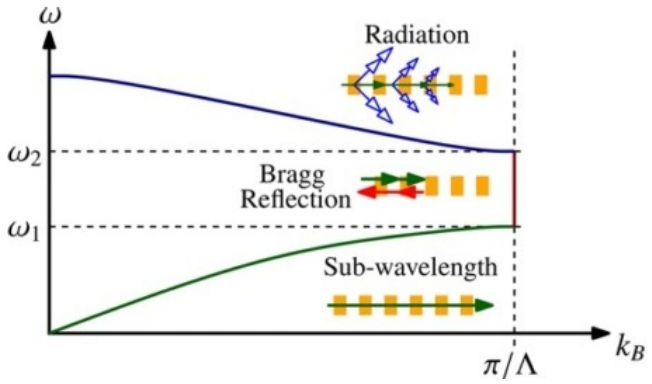

Figure 2.1: Dispersion relation of 1D

Figure 2.1 shows a schematic (k-ω) diagram of a 1D periodic structure [1]. One can see that, for a given periodicity of the structure, the working regime is strongly related to operating wavelength Îż or operating frequency ω. When $\omega > \omega_2$ (above the first photonic bandgap), the waveguide becomes lossy for Bloch mode, and the light will be radiated out of the waveguide. This character has been utilized to design fiber-to-chip surface couplers (grating couplers). In the frequency range of $\omega_2 > \omega > \omega_1$ (the

first photonic bandgap), light cannot propagate through the periodic structure and is reflected backward, and this is Bragg reflection regime. The propagation constant in this regime is $K_B = \pi/\Lambda$. The bandgap has been extensively exploited to design distributed Bragg reflectors (DBRs) on different photonic platforms. The last regime where operating frequency is below ω_1, propagation constant k_B grows monotonically as operating frequency increases, indicating that the periodic waveguide behaves as a conventional waveguide. Thus in sub-wavelength regime periodic structure work as a homogeneous media.

2.2 SWG waveguide in SOI

In this work Sub-wavelength grating (SWG) waveguide is preferred [for filter characteristic than DBR ?]over conventional waveguide due to its extra degree of freedom on waveguide property tuning as mentioned in chapter 1. Light propagates in SWG waveguide by suppressing reflection and diffraction effects only when SWG period (Λ) is sufficiently small compare to operating wavelength (λ) so, by having different materials combined at a sub-wavelength scale can be approximated as a homogeneous effective medium similar to conventional waveguide but the difference is light propagates as a Bloch mode in SWG waveguide because of periodic structure [see figure]. The wave propagation in periodic media can understood from Bloch theorem which is been widely used in solid state physics . The same concept can be used to study the electromagnetic wave propagation in a periodic dielectric medium. The propagation of Bloch mode through z periodic waveguide can be expressed as

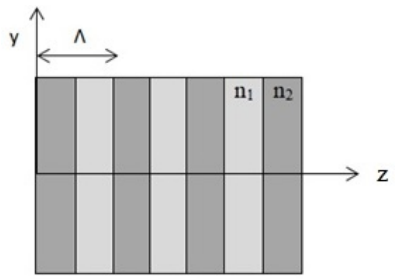

Figure 2.2: Schematic of a 1D periodic medium consisting of tow alternating material layer of refractive indices n_1 and n_2

$$\vec{E} = \vec{E_K}(z)e^{j(\omega t - k_y y)}e^{-jKz} \tag{2.1}$$

Where E_k is a periodic function with period Λ, k_y is a wavevector component along y direction and ω is angular frequency.

$$\vec{E_K}(z) = \vec{E_K}(z + \Lambda) \tag{2.2}$$

where the constant K is the Bloch Wave number.

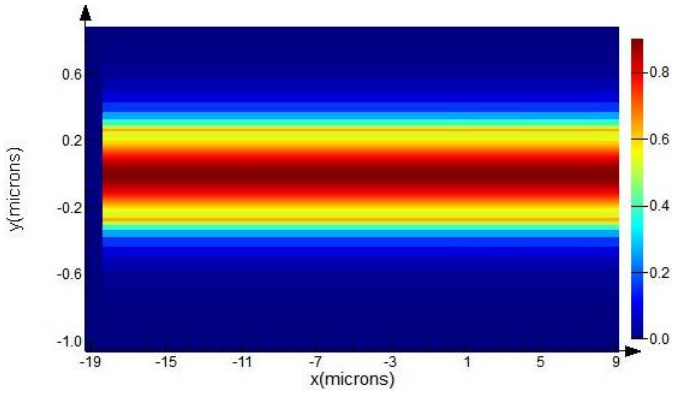

Figure 2.3: Strip waveguide

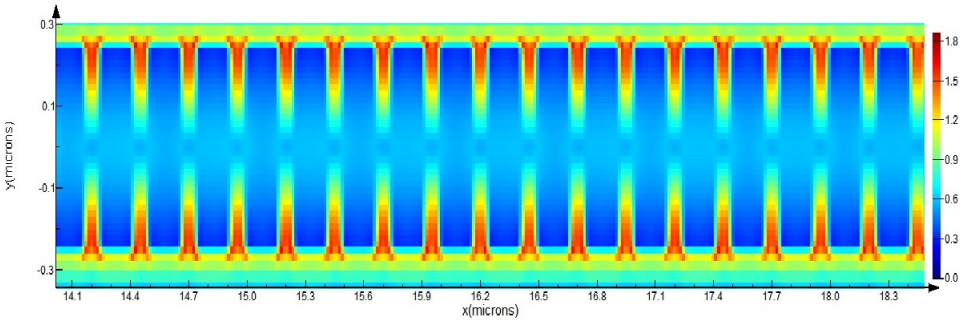

Figure 2.4

SWG waveguide in SOI, can be realized by having periodic arrangement of high and low refractive index material as shown in figure 2.2. where W,H and Λ are width, hight and period of SWG. The effective refractive index however can be adjusted by period, duty cycle of SWG and therefore can be optimized for given application.

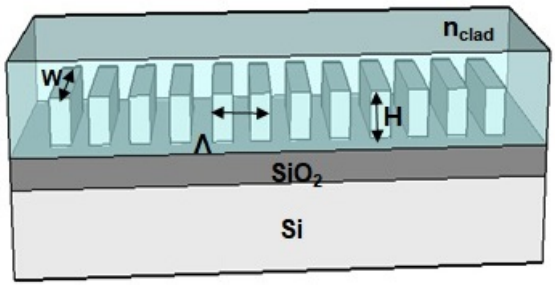

Figure 2.5: SWG waveguide in SOI

2.3 Single mode waveguide in SOI

In most application, waveguide are required to support a single mode if not the presence of higher order modes will lead to unwanted peaks in transmission spectrum which are undesirable therefore low loss and minimum inter-modal dispersion is achieved in single mode waveguide. Traditional SOI waveguides have a typical propagation loss of about 3 dB/cm [], that can be reduced up to 0.7 dB/cm [] Standard strip waveguide which supports single mode in the 1550 nm telecommunication window have rectangular cross-section (220 nm high and 500 nm wide), supporting TE and TM polarized fundamental modes [3,5]. The height(H) and width (W) of Strip Waveguide and fully etched SWG waveguide are fixed throughout this work.

2.4 Design of SWG waveguide and taper

In order to exploit the flexibility afforded by SWG waveguide, it has to be integrated and interconnected with conventional waveguide. But this requires adiabatic taper to do because the modes of strip and SWG waveguides are very different, without adiabatic taper it would cause unwanted extra loss. To avoid an abrupt transition, in literature we have design of SWG taper where it works with gradual modification of SWG effective refractive index for a smooth transition from a SWG mode to a strip mode (or vice versa) and to adjust adiabatically the mode size. This is achieved by chirping the grating period and duty cycle.To generate a smoother transition from SWG to strip waveguide, bridging silicon elements are added in the taper structure, between SWG silicon blocks, so the equivalent refractive index is progressively increased to match strip n_{eff}. Figure

shows SWG taper[] where taper end width varies from 100 μm to 150 μm and taper length varies from 15 μm to 50 μm.

Figure 2.6: Top view of SWG Taper form 3D FDTD simulation []

In order to understand the deciding factors for light guidance in SWG waveguide and the requirement of SWG taper, a three-dimensional (3D) finite-difference time-domain (FDTD) simulation on SWG waveguide was performed to get a pass band nearλ = 1550 nm wavelength which is a part of simulation work as obtained in the paper titled "Sub-wavelength grating components for integrated optics applications on SOI chips"[] is been reproduced. The design parameter for SWG waveguide were chosen such that grating period Λ less than a half of the effective wavelength of waveguide mode λ_{eff} = /2n_{eff}.All the simulation was done with a mesh resolution of Δx $\times$ Δy $\times$ Δz = 15 $\times$ 15 $\times$ 15 nm^3 and Perfectly Matched Layer (PML) boundary condition is been used so that radiation appears to propagate out of the computational area and therefore, does not interfere with the fields inside. Material refractive indices used are n_Si = 3.476 for the waveguide core, n_SiO = 1.444 for the waveguide lower cladding (bottom oxide, BOX), and n_{Air} = 1 for the waveguide upper cladding []. Figure shows the top view of the simulation structure consists of a 20 μm long SWG waveguide with a grating period Λ = 250 nm, duty cycle δ = 0.7, width of the segment w = 220 nm and segment length a = 175 nm. The Strip waveguide (width 220 nm) waveguide mode is used to excite the SWG waveguide Bloch mode at λ= 1550 nm through SWG taper length of 15 μm. TE fundamental mode with wavelength range from 1.3 μm-1.9 μm is been launched as a source in the input waveguide and propagate through SWG waveguide by SWG adiabatic tapering and the transmission spectra is been collected at the output waveguide by frequency domain field and power monitor(o/p monitor) as shown in figure 2.7.

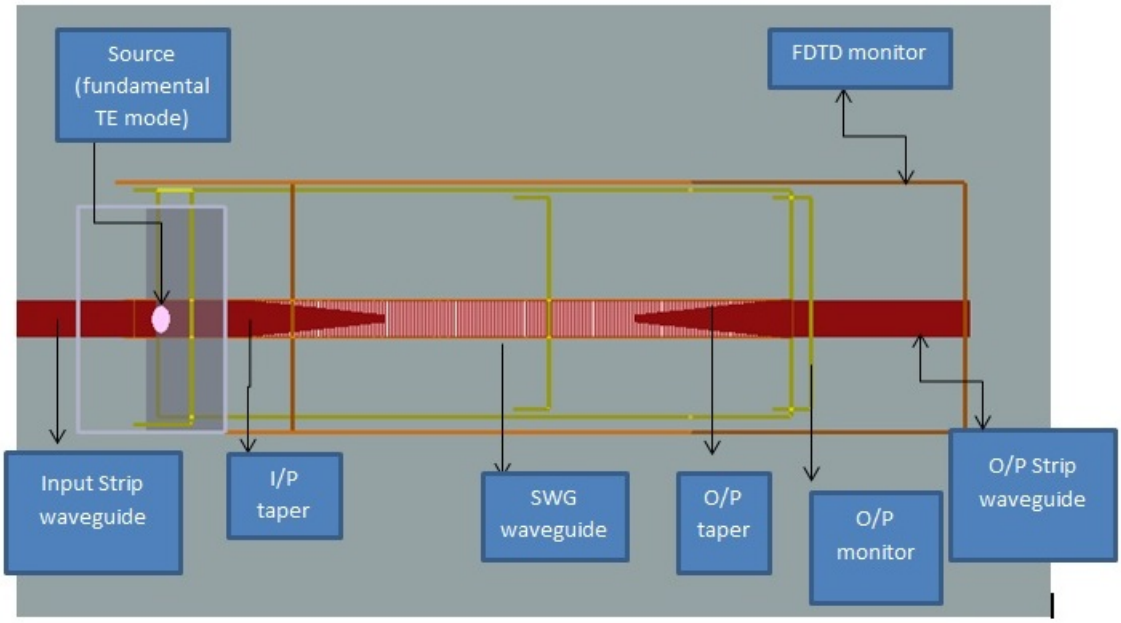

Figure 2.7: Top view of SWG Waveguide from FDTD Simulation

2.5 Result and Discussion

Figure 2.8 (a) and (b) represents the transmission spectra of SWG waveguide with duty cycle 0f 0.7 and 0.5. The light guidance in SWG waveguide with air as a upper cladding have a higher cut-off with duty cycle value. For SWG waveguide with duty cycle of 0.5 gives no transmission [see figure 2.8 (a)] because the evanescent field penetrates deeper in the upper cladding when the SWG duty cycle is smaller, thus a reduced duty cycle means that light confinement in the core is decreased therefore we observe no guidance in the SWG waveguide. But for the duty cycle of 0.7 the refractive index contrast between SWG waveguide and upper cladding is been increased such that it can support a mode in the waveguide therefore a passband for wavelength range 1.35 μm to 1.6 μm is been obtained and this falls in sub-wavelength region where it lies below the Bragg wavelength. And beyond 1.6 μm wavelength the transmission drops because of the lower cutoff where it lies below the light-line of sio_2 which can be understood from band structure plot as shown in figure 2.8 (C) where the light green dotted lines indicate light-line of cladding region here we see it for sio_2 (lower cladding), the guided mode should be above the light-line of upper and lower cladding material if not it leaks to the cladding region. In our case beyond 1.6 μm wavelength (188 THz) the guided modes leaks to the lower cladding sio_2, it conforms that result obtained from FDTD solution

for transmission spectrum matches to the band structure calculation. As we move from SWG region to Bragg region, it should be a smooth transition if not we see more peaks due to fabry-perot effect near the band edge at 1.3 μm wavelength in the transmission spectra this can be reduced by increasing the taper length in input and output waveguide side.

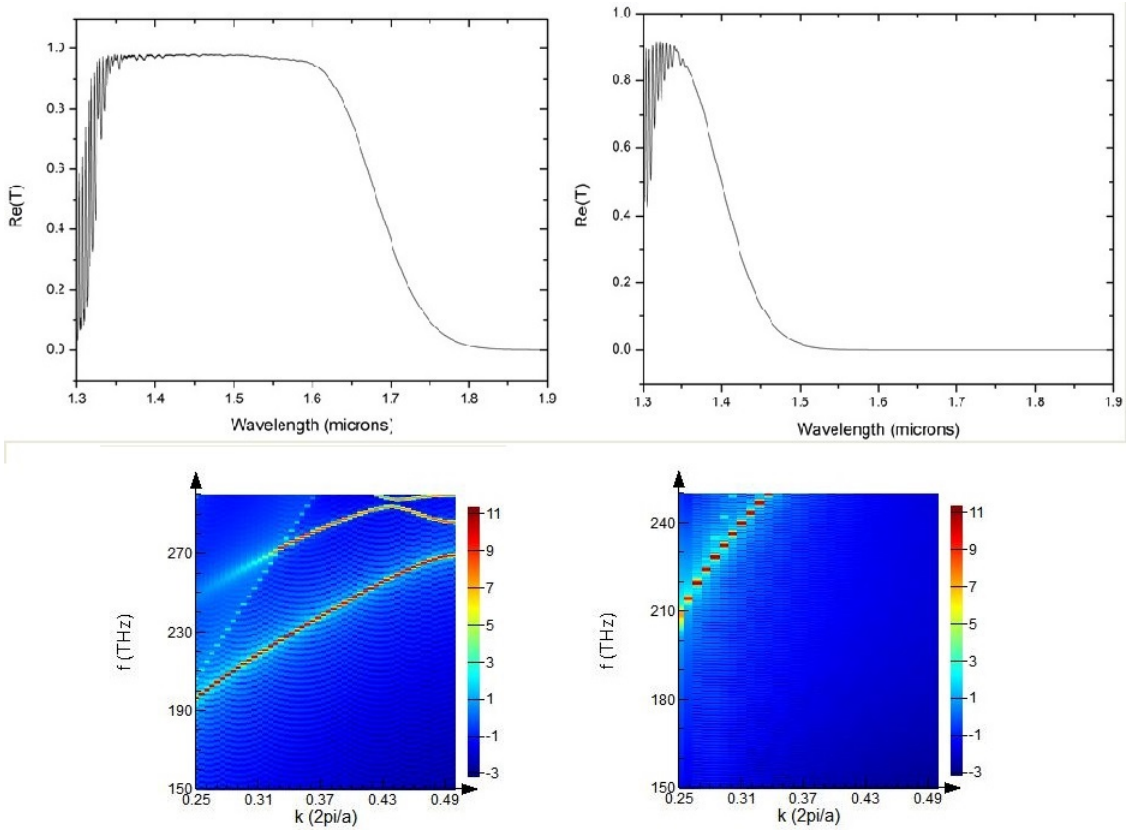

Figure 2.8: Transmission spectra for SWG waveguide (a) with duty cycle of 0.7 and (b) with duty cycle of 0.5, band structure plot for SWG with (c) duty cycle of 0.7 and (d) duty cycle of 0.9

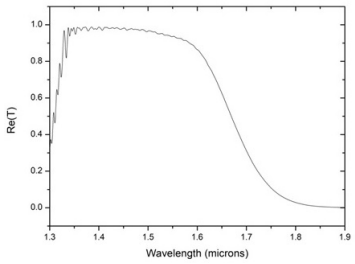

Figure 2.9

figure 2.9 :With one side taper we observe that F-P effect is been reduced therefor by having proper design of taper lead to avoid peaks near the bandedge where have transition from SWG region to Bragg region.

CHAPTER 3

Results and Discussion

3.1 Simulation results

As discussed in the previous chapter, from SWG waveguide we get a broadband spectrum the bandwidth of passband obtained for those design parameter was 200 nm. But to have a passband edge near 1550 nm wavelength we need to increase the period (Λ) and duty cycle δ of SWG. In this chapter we will discuses the simulation result for effect on period and duty cycle change in transmission spectrum of SWG waveguide and understand how SWG Waveguide act as a Fabry-Perot cavity for some period and how SWG taper behaves as a reflector. Then we move to our propose structure to overcome all this drawbacks.

3.1.1 Effect of period change in the SWG

As we shift from period (Λ) 250 nm to 350 nm and all other parameter same for the structure in figure 2.7 we expect red shift in the pass band edge ($\lambda = 2n_{eff}\lambda$) which is observed near 1.3 μm wavelength in the transmission spectra and photonic bandgap is been observed form 1.3 μm -1.32 μm wavelength but with additional to it we observe extra bandgap from 1.35 μm to 1.6 μm which falls in sub-wavelength regime [see figure 3.1 (a)] which is not the expected result because SWG waveguide transmit incoming wavelength only when it is much larger than the period of SWG. Even though SWG mode guidance condition is satisfied, a bandgap is observed in the sub-wavelength regime. To understand the extra bandgap creation in the transmission spectrum, a simulation was done by removing input and output taper in the structure as shown in figure 3.3.

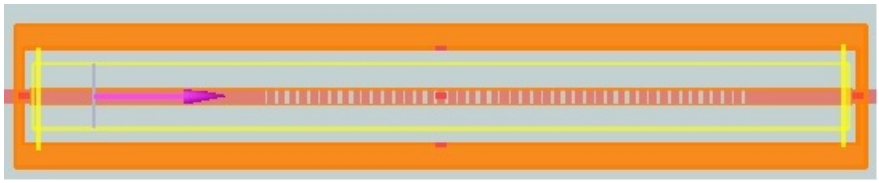

Figure 3.1: Top view of SWG waveguide without SWG taper

Result and discussion

Figure 3.1 (b) represent the transmission plot for the SWG waveguide with absence of taper in the input and output waveguide. The output power level decreases in the transmission spectra due to abrupt transition from strip to SWG waveguide (vice versa) therefore by having taper in both side of waveguide reduces mode mismatch and n_{eff} mismatch this difference can be seen between figure (a) and (b). A bandgap is been observed between 1.3 μm to 1.32 μm wavelength which falls in the Bragg region which also conforms with bandstructure calcuation [see figure 3.2]

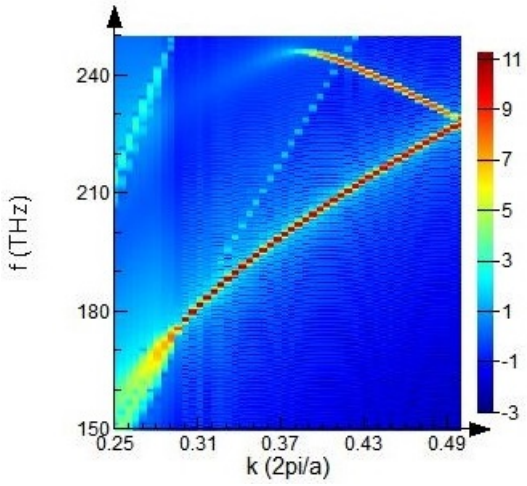

Figure 3.2: Bandstructure plot for period Λ = 350 nm and duty cycle δ = 0.7

And above the bandgap wavelength we can observe the sub-wavelength transmission region which is not observed in the figure 3.3 (a), so this confirms that presence of SWG taper give rise to additional bandgap and partial Fabry-Perot effect due to which we observe more unwanted peaks in the transmission near the bandedge for 350 nm period.

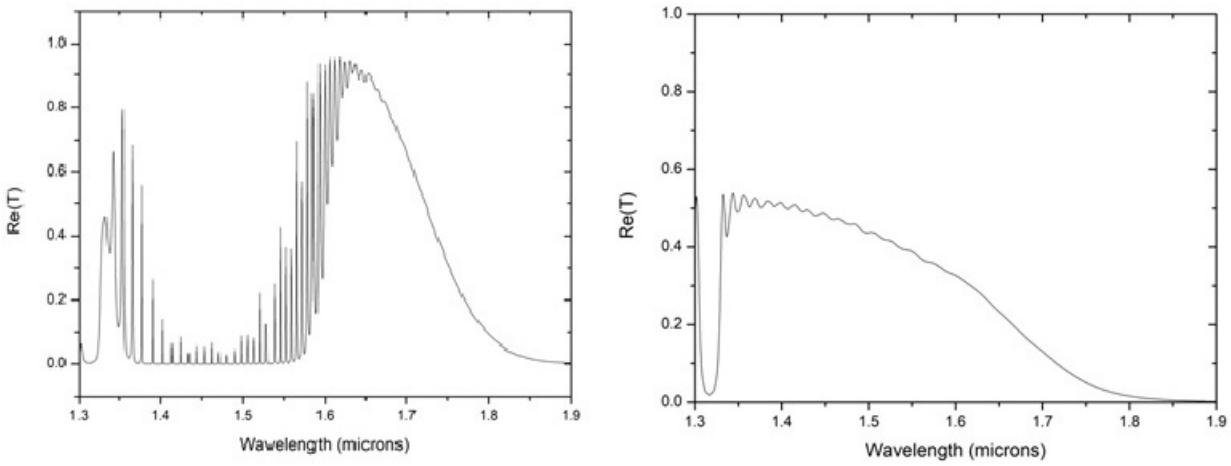

Figure 3.3: Transmission spectra for SWG period 350 nm: (a) with SWG taper, (b) without SWG taper

3.1.2 Proposed Work

SWG taper with period 350 nm results Fabry-perot effect and a bandgap which was absent for period 250 nm. To understand the cause of it we modified the structure as shown in figure where we removed the SWG waveguide (center region) which was acting as a cavity and joining input and output taper together through SWG. We simulate this structure in 3D FDTD for two different taper length and study there transmission response.

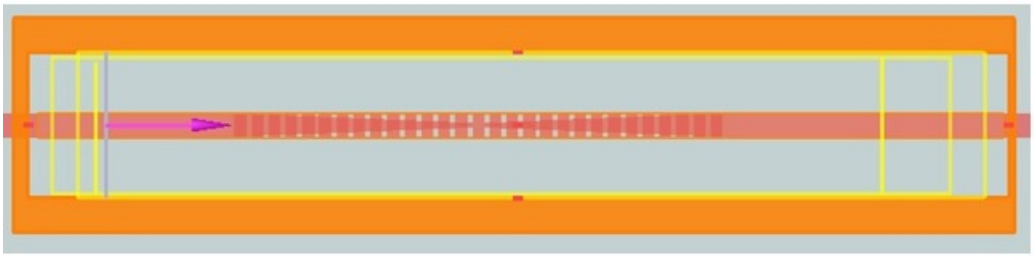

Figure 3.4: Top view of SWG taper

3.1.3 Taper length variation

SWG structure [see figure 3.3] for two different taper length with period 350 nm and duty cycle of 0.7 is been simulated to understand reflection of certain wavelength from SWG taper. Later we discuss the effect of change in duty cycle for each taper length in the transmission spectra

Taper length 10 μm

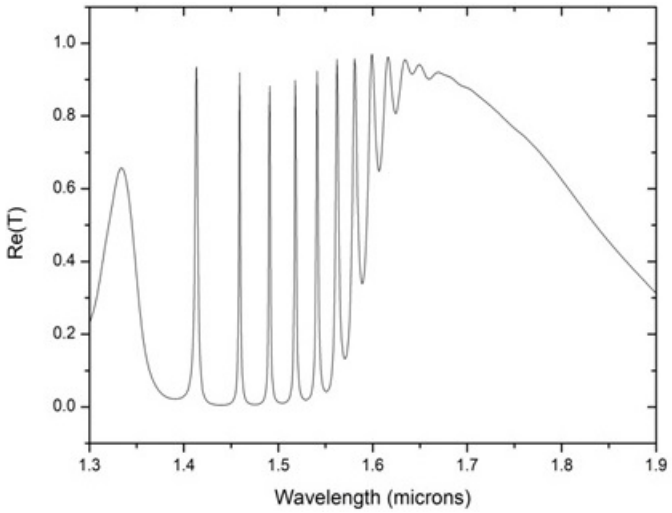

Figure 3.5: Transmission spectra for period 350 nm and duty cycle 0.7

The input and output taper are no more SWG it acts as a Disturbed Bragg grating (DBR) and results Fabry-Perot resonances in the transmission spectra of figure 3.4. On understanding how light propagates in the proposed structure will lead to clear explanation of the figure 3.4. We can consider the structure in figure 3.3 as three Separate DBR region : DBR 1, DBR 2 and DBR 3 as shown in figure 3.5. We see that DBR 1 and DBR 2 have same n_{eff} because the tapering on both side is the same where as in DBR 2 region the n_{eff} is different and smaller than other two region because of reduction in taper width. Since DBR 1 and DBR 2 have same Bragg wavelength and see the DBR 3 region as a cavity, in cascaded effect of all three and starts reflects back and forth as a result we see resonance peak in the transmission spectra. DBR 3 region does not see any cavity, so its spectrum pass through the taper structure and its Bragg wavelength is smaller than other two so as it pass through the taper region it interfere with the spectrum of DBR 1 and DBR 2 whose left bandedge wavelength coincide with the DBR 3 right bandedge as a result we see no ripples at the left edge of the band in the transmission spectra. The other side of the pass band falls because of the upper cutoff of the guided mode where it cross the light line of Sio_2 at higher frequency and leaks to substrate. At longer wavelength near 1.6 μm the transmission drops and leaks to the substrate because it cross the light line of sio_2 at lower frequency

On achieving a Fabry-Perot resonance peak, further analysis is to increase the qual-

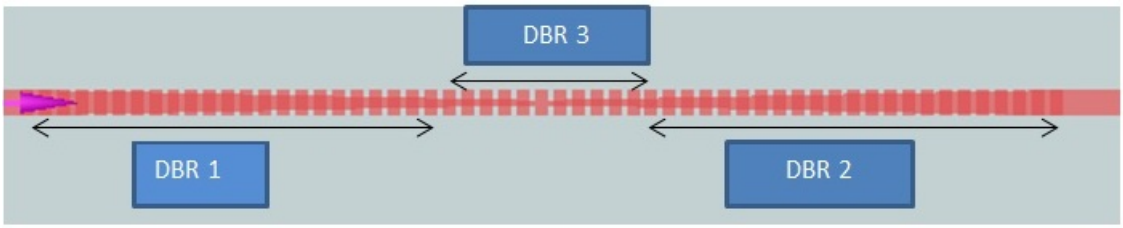

Figure 3.6

ity factor (Q) of the peak which is defined as ration of resonate wavelength of the peak to the 3-dB bandwidth and analysis the narrow passband with change in duty cycle.

Duty cycle variation

Figure 3.6 represents the effect of change in duty cycle on transmission spectra for taper length 10 μm. As duty cycle increases from 0.7 to 0.9, the passband becomes flat top, increase in bandwidth around 100 nm and output power level increase due to n_{eff} contrast level in the core increases with the duty cycle as result we get high power level in figure 3.6 (b).

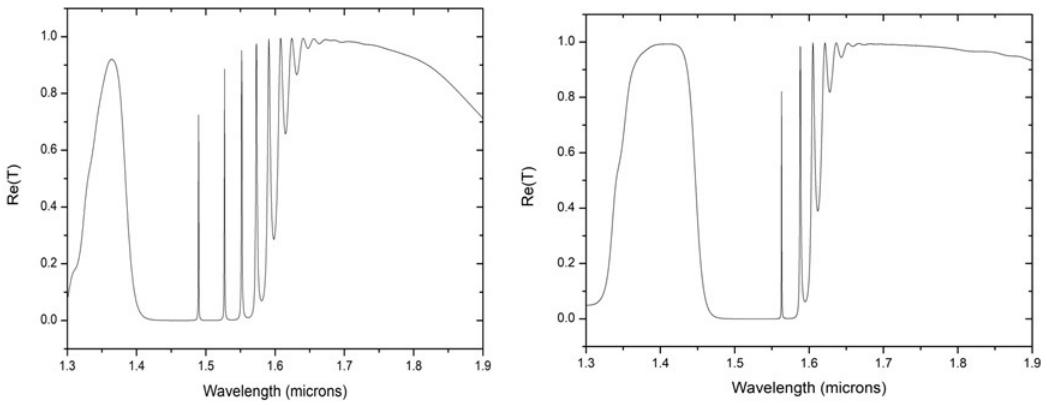

Figure 3.7: Transmission spectra for period 350 nm : (a) duty cycle 0.8 and (b) duty cycle 0.9

By increase in duty cycle the resonant peaks have also reduced due to suppression of Fabry-Perot effect near to the right edge of the band and also Q value increase with duty cycle, for 0.7 it is less than 1000 but at 0.9 Q value is very large since it would not be calculated with the simulation due to requirement of large data points which consumes so many days, therefore precoded with analysis of variation of taper length.

Taper length 20 μm

For taper length of 20 μm with all other parameter same we get transmission spectra as shown in figure 3.8 and 3.9. By comparing it with taper length 10 μm the resonant nature of the device as been reduced for duty cycle of 0.7 and we get a similar transmission spectra which is been obtained with our previous design where we have SWG waveguide in the design.

Result and discussion

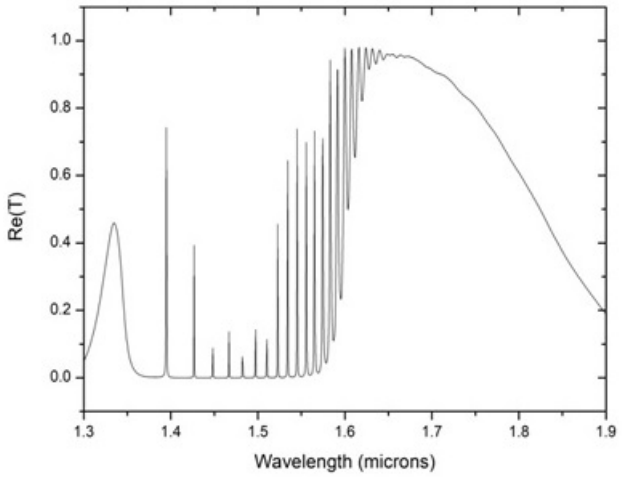

Figure 3.8: Transmission spectra for Taper length 20 μm: Λ = 350 nm, δ = 0.7

For duty cycle of 0.9 we get a sharp bandedge in the left edge of the band which is due to suppression of Fabry-Perot effect in the left edge band. When all three DBR region cascaded, the spectrum of all three region is such that we obtain a overlap between right edge of band of DBR3 with the left edge of band DBR 1 and DBR 2 as result we see sharp left edge band in the transmission spectrum [see figure 3.8]. The other side of the pass band edge have a slope nature because it cross the light line of sio_2 at higher frequency and leaks to substrate. We see peaks in the right edge of the band near 1.6 μm wavelength due to mis overlap between DBR 1, DBR 2 right edge band with DBR 3 spectrum and beyond 1.6 μm wavelength we see sub-wavelength region.

As we increase the duty cycle from 0.7 to 0.9 we see decreases in the band gap this is because the n_{eff} of SWG increases so the coupling between forward and backward mode is less as a result we see reduced bandgap but this argument does not much with

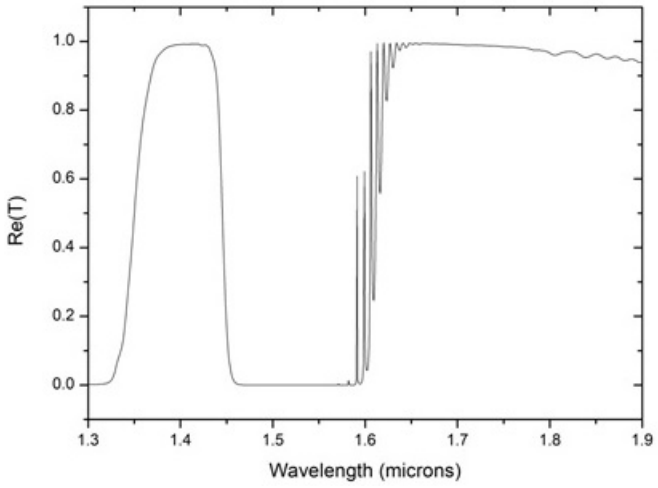

Figure 3.9: Transmission spectra for Taper length 20 μm: Λ = 350 nm, δ = 0.9

the bandstructure plot [see figure 3.10]

Analysis of bandstructure with variation of duty cycle

The duty cycle variation of SWG results more refractive index contrast between core and cladding material as a result we see less resonance peaks in the transmission spectrum for higher duty cycle and also we get high output power level. To understand how duty cycle parameter plays role in the light guidance in the SWG waveguide and also in the photonic bandgap region, bandstructure simulation was performed in the FDTD by considering only the SWG region and choosing boundary condition in periodic direction as Bloch and other direction as PML boundary.

Result and Discussion

Figure 3.10 shows bandstructure plot for duty cycle variation for period Λ = 350 nm. As duty cycle increase from 0.5 to 0.7 we see the guided mode red dotted lines move away from the light line of sio_2 and we get complete guides in the SWG region for duty cycle 0.7, but due to Bragg reflection from the taper the SWG region is not observed for this period in the transmission spectra as discussed in figure 3.3 (a), and also the photonic bandgap decreases for this increase in δ and at δ = 0.7 the bandgap becomes narrow (2 μm) which was observed in the figure 3.3. Beyond δ = 0.7 we see the bandgap becomes wider and for 100 percent duty cycle we see no bandgap as expected for strip

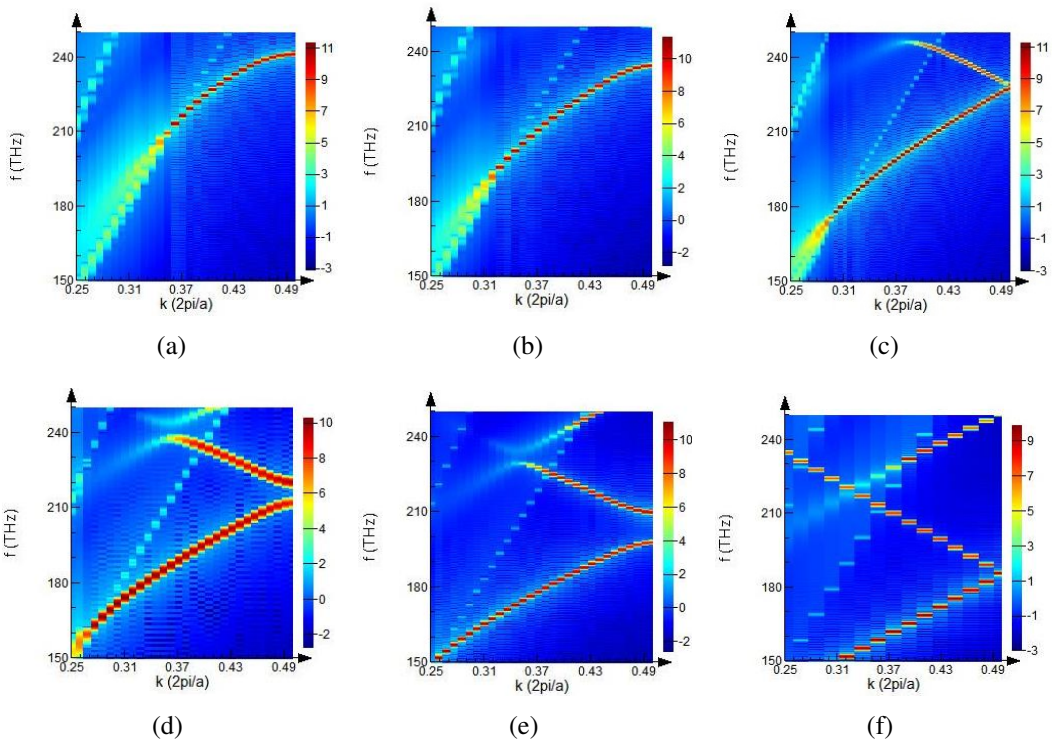

Figure 3.10: Bandstructure plot for period Λ = 350 nm: (a) duty cycle of 0.5, (b) duty cycle of 0.6 (c) duty cycle of 0.7 (d) duty cycle of 0.8, (e) duty cycle of 0.9, (f) duty cycle 1

waveguide.

The results of bandstructure plot matches with the transmission spectra of abrupt junction structure [see figure 3.1] and the results are compared for two different duty cycle value one is 0.7 and other is 0.9 because to analysis the extreme case . From figure 3.11 we can observe that band gap becomes wider and spectrum shift to higher wavelength with high output power level due to increase in n_{eff} as δ change from 0.7 to 0.9. For (b) we observe that it near band edge more ripples due to abrupt change from one region to other region in dispersion plot.

With the presence of taper structure, transmission through SWG waveguide would not be explained with the bandstructure plot because for Λ = 350 nm, the taper acts a DBR grating and the SWG waveguide as cavity therefore the light propagation in device [see figure 3.4] is explained through figure 3.6 where we considered cascading of three DBR structure.

Figure 3.12 represents the transmission spectra of two different structure as seen

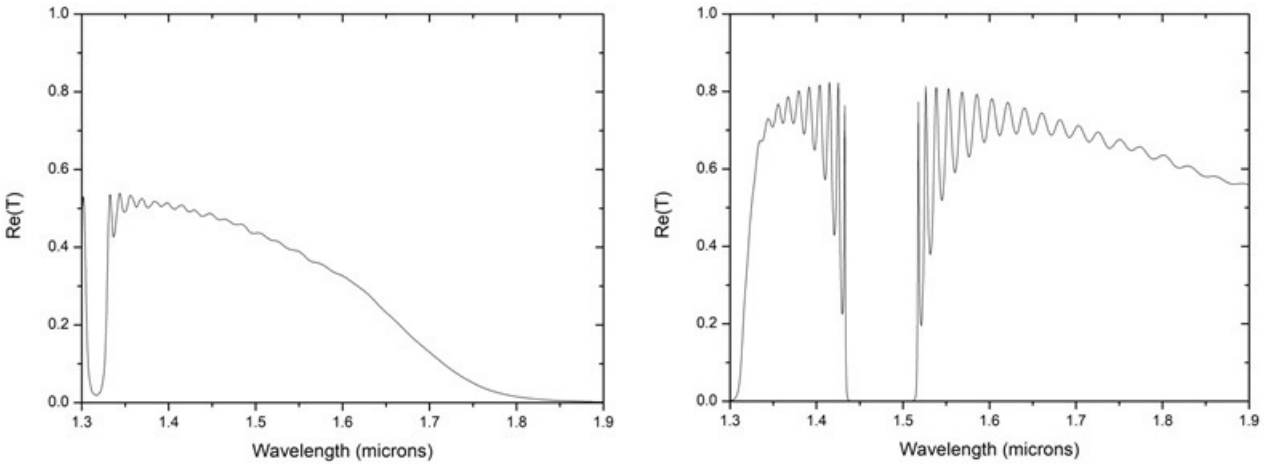

Figure 3.11: Transmission spectra for Taper length 20 μm: Λ = 350 nm, δ = 0.9

earlier, (a) and (b) represents the transmission for the structure in figure 2.7 where we have SWG waveguide between input and output taper and (c) and (d) represents the transmission for structure in figure 3.4. As we can see that with the presence of taper dominates over the SWG waveguide because the transmission spectrum obtained with absence of SWG waveguide give same response as with presence of SWG waveguide therefore the incoming light see only the effect of taper only with SWG waveguide we get not much difference, so proposed structure gives sharp left edge pass band by suppressing Fabry-Perot effect which can be used for filter characteristic and by shifting the period from 350 nm to 450 nm we can get pass band near 155o nm.

Concept of taper was to neglect the abrupt transition from strip to SWG waveguide (or vice versa) and achieve a smooth transition but as we have seen for Λ = 350 nm it modifies the band edge for higher duty cycle . The abrupt transition structure and proposed structure is been compared so that to get the clear picture of taper action in the transmission spectra In figure 3.13, (a) and (b) represents the two different structure with Λ = 350 nm and δ = 0.9 and total device length of two structure is 40 μm , (a) abrupt transition structure in figure 3.3: we see more ripples in the band edge and not flat top pass band is been achieved but by having tapering from strip to SWG as shown in figure 3.4 r we achieve sharp left edge and flat top pass.

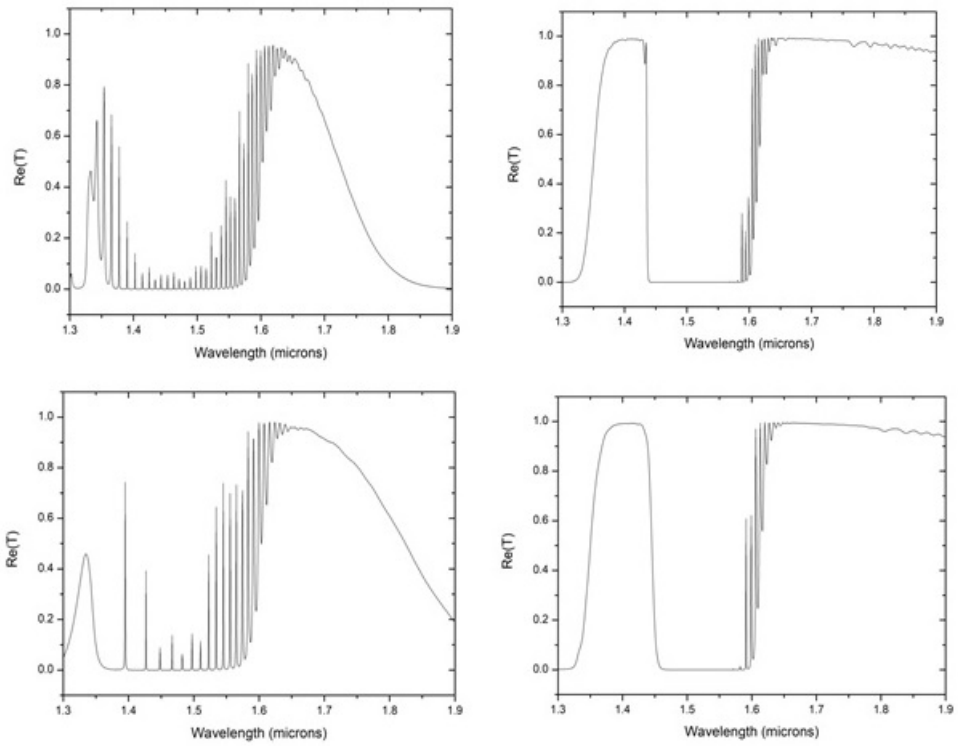

Figure 3.12

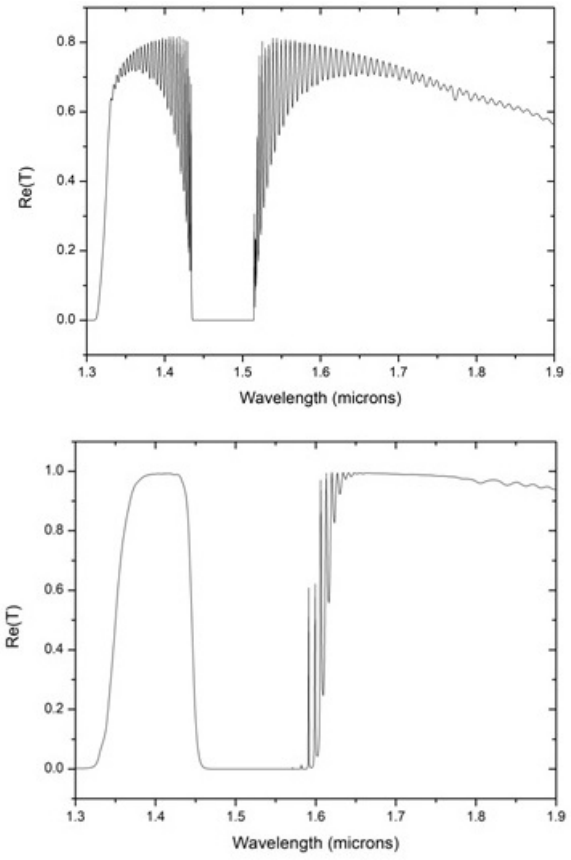

Figure 3.13

CHAPTER 4

Conclusion

4.1 Summary

The SWG waveguide parameter period (Λ), duty cycle (δ) is been varied to study the transmission spectra and the bandstructure of SWG. In the process we understand the working principle of existing SWG waveguide structure and and SWG taper design as seen in chapter 2 the abrupt transition structure (absence of taper) was simulated and lead to conclusion that SWG taper plays role in reduction of mode mis-match and extra.Further for chandge in period results Fabry-Perot effect in the transmission spectra due to SWG taper which was confirmed with bandstructure plot and also from the abrupt structure. To increase the Fabry-Perot effect and to neglect it completely the proposed structure was simulated for different taper length, for shorter taper length we observe hight quality factor and it increase with change in duty cycle. For longer taper length with higher duty cycle we obtain sharp left edge and flat top pass band. Bandstructure plot for SWG with duty cycle variation was observed in chapter 3. The plot helps to understand how photonic bandgap changes with duty cycle and from the results of abrupt structure the transmission spectra matches to the bandstructre plot. And the taper effect on transmission spectra is been analyzed between proposed structure and the abrupt transition structure.

4.2 Outlook

The proposed device will definitely serve as a good candidate for sharp edge filtering application and with a combination of shorter taper length with high duty cycle will lead to high quality factor which can be used in add-drop porr of microring resonator structure. It can be used in the refractive index sensing application like lab-on chip sensor.